Influences of particle characteristic and compaction degree on the shear response of clinker ash

Michael James Winter[a], Masayuki Hyodo[a], Yang Wu[a,*], Norimasa Yoshimoto[a], Muzamir Bin Hasan[b], Kanta Matsui[a]

[a] Graduate School of Science and Technology for Innovation, Yamaguchi University, Ube, Japan
[b] Faculty of Civil Engineering & Earth Resources, University Malaysia Pahang, Malaysia

ARTICLE INFO

ABSTRACT

Clinker ash is regarded as a granular waste of coal combustion but potentially employed as a recycled and light-weight backfill material for retaining wall and embankment in recent years. The physical, particle, compaction and mechanical properties of six selected types of clinker ash were thoroughly examined in this experimental investigation. Clinker ash owns very complex and angular shapes and it gives rise to the larger difference between the maximum and minimum void ratios. The single particle crushing strength of clinker ash is around 1/5–1/10 lower than natural sands and it indicates high crushability in nature. With similarity to natural sands, the mean crushing strength of clinker ash displays a decreasing tendency with the increase in grain diameter. A series of triaxial compression tests were performed on different types of clinker ash to examine the influences of particle characteristics, degree of compaction and effective confining pressure on their shear behaviour and deformation characteristics. Test results demonstrate that clinker ash possesses a higher peak friction angle at low effective confining pressures and gradually loses its shear strength with the rise in effective confining pressure. The great shear strength dependence on the stress level for clinker ash is confirmed. The stress-dilatancy behaviour of a given type of clinker ash is minimally affected by the degree of compaction and level of effective confining pressure. The stress ratios at the critical state of clinker ash are well correlated with the mean crushing strengths. A larger N value for clinker ash determined using Nova's rule indicates its higher crushability. The downward shift of critical state line of clinker ash due to grain crushing is identified on the void ratio and logarithm of effective mean stress plane. Additionally, grain crushing was confirmed by the comparison of the variation in grain size distribution curves and the observation of colored particles previously seeded in the tested samples before and after shearing.

1. Introduction

Coal has been employed widely as an energy resource around the world for a very long time due to its vast amount of storage and low cost. Coal is recognized as an alternative energy resource for the nuclear and petroleum oil for the integrated energy strategy of Japan. Currently, a large amount of coal are being used by thermal power plants to supply power through incineration of coal. This in turn leads to a remarked rise in the generation of coal ash in high quantities. In recent few years, the total amount of coal consumption for thermal power plants in Japan is continually increasing due to the rise in energy demand and shutdown of nuclear electricity generation after the 2011 Great East Japan earthquake. Accordingly, that makes the increasing amount of waste in accompaniment with coal combustion much worsen. The total amount of coal ash produced by coal-burning power

plants was 12.62 million tons in Japan in 2014 according to the survey by Japan Coal Energy Center (Jcoal, 2014).

Fly ash and clinker ash account for majority of the coal ash during coal combustion. Fly ash is composed of light and fine coal ash particles that float into the exhaust stacks. Clinker ash, also called bottom ash, is the coarser component of coal ash particles and collected from the bottom of boiler. Fly ash with the light form, around 85%–95% of generated coal ash, had been effectively utilized as an additive into cement to manufacture concrete and ground materials for construction projects (Chang et al., 1977; Chiaro et al., 2015; Ferreira et al., 2003; Iyer and Scott, 2001; Kamon et al., 2000; Lee et al., 2003; Trivedi and Sud, 2002; Wang et al., 2013; Yilmaz, 2015; Yoshimoto et al., 2012). However, clinker ash, which makes up around 5–15% of generated coal ash, is still not being recycled effectively. Disposal of unused clinker ash as pond and landfill gives rise to significant socio-economic and

environmental problems. For the domestic conditions in Japan, a new law to ensure the recycling of materials by society named "The Basic Law for Establishing the Recycling-based Society" was enacted in 2001 (Ministry of the Environment, 2000), and following this other laws related to the environment protection were revised and implemented one after another. Particularly, coal ash was designated as a "specified by-product for which the effective use as a recycled resource should be promoted" in the "Law for Promotion of Effective Utilization of Resources" (METI, 2000). It was specified in "Law on Promoting Green Purchasing" that the high rate of reuse of coal ash was not enough for public works and the effective recycling of clinker ash was vigorously advocated. Therefore, efficient and effective methods for treatment and reuse of clinker ash still require further investigation.

Although some previous investigations were undertaken to study the engineering characteristics of fly and bottom ash mixtures (Jayaranjan et al., 2014; Kim et al., 2005; Latifi et al., 2015; Yoon et al., 2009). However, limited study on the engineering properties of pure clinker ash as geomaterial had been reported in the literature. Arakawa et al. (2004) examined the applicability of clinker ash for soil improvement. Consoli et al. (2007) studied the shear behaviour of bottom ash produced in Brazil at vary small to very large shear strains and reported that bottom ash had a higher shear strength but a lower stiffness than other typical sands. Wakatsuki et al. (2009) examined the monotonic and cyclic behaviours of clinker ash at loose state and noticed that the shear strength and liquefaction resistance of clinker ash were higher than natural sands. Kim and Do (2012) investigated the effect of particle size on the frictional resistance of bottom ash-added composite geomaterial. Winter et al. (2015) proposed an empirical equation to estimate the shear strength of clinker ash based on a series of test results considering the influences of stress, density and particle shape but not examined the deformation behaviour of clinker ash. However, the physical and engineering properties of clinker ash are still not thoroughly investigated. This deficiency makes the wide application of clinker ash as backfill materials for construction projects a difficult task.

This study aims to investigate the physical, particle, compaction and mechanical properties of clinker ash. Six types of clinker ash are collected from different coal-burning power plants and tested to provide a better wide of results and understanding of the mechanical behaviour of clinker ash. A series of drained triaxial compression test were performed on six types of clinker ash under varying effective confining pressures and degrees of compaction to understand their influences on shear strength and deformation behaviour. Additionally, the influence of degree of compaction on the stress-dilatancy relationship and critical state characteristics are also examined. Comparison of grain size distribution curves before and after shearing and observation of the colored particles seeded in the specimen in advance of testing are conducted to confirm the occurrence of particle breakage for clinker ash during shearing.

2. Physical, particle and compaction properties of clinker ash

2.1. Physical properties

Clinker ash is the granular waste by-product that results from the operation of coal-fired power plant. Totally, six types of clinker ash samples are collected from thermal power plants in western Japan and named as CA, CB, CC, CD, CE and CF in this study. C represents the initial characteristic of clinker. A, B, C, D, E and F stand for the type of clinker ash from different sites. Table 1 shows the physical and particle properties of six types of clinker ash. The clinker ash owns a particle density ρ_s varying from 2.072 to 2.173 g/cm^3 which is lower than natural sands (density between 2.6 and 2.8 g/cm^3) and is regarded as a light-weight granular material. This is caused by the grain internal structure containing irregular air vesicles.
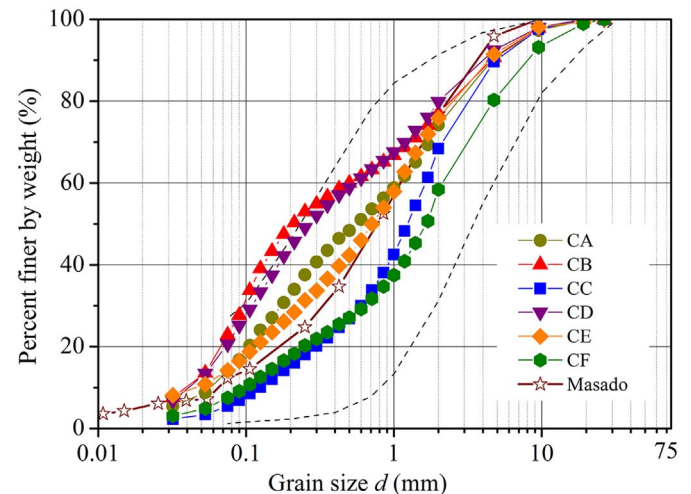
Fig. 1 shows the grains size distribution curves of the six types of

Table 1
Physical and particle properties of different types of clinker ash.

Sample	ρ_s (g/cm^3)	e_{max}	e_{min}	U_c	d_{50} (mm)	A_r	R_c	σ_{fm} (MPa)
CA	2.072	1.748	0.949	20.3	0.57	1.55	2.73	4.27
CB	2.151	1.646	1.010	12.5	0.21	1.46	2.55	1.99
CC	2.173	1.618	0.883	13.8	1.3	1.42	3.04	2.56
CD	2.132	1.488	0.887	21.2	0.22	1.60	3.39	1.04
CE	2.151	1.422	0.752	26.7	0.71	1.45	2.63	4.75
CF	2.110	1.425	0.769	21.0	1.75	1.40	2.55	3.12

ρ_s particle density; e_{max} maximum void ratio; e_{min} minimum void ratio; U_c coefficient of uniformity; d_{50} median diameter; A_r aspect ratio; R_c roundness coefficient; σ_{fm} mean crushing strength.

Fig. 1. Grain size distribution curves of different types of clinker ash.

clinker ash. The grain size distribution is measured following the standard specification in (JIS A 1204, 2015). The region between two broken curves without symbol represents the range of results on 60 different types of clinker ash gathered from 15 thermal power plants in Japan (Wakatsuki et al., 2009). The grain size distribution curves of the samples used in this research give a good representation of the overall particle distributions of clinker ash. The grain size distribution of clinker ash is wide and varies with the location site, performance of the boiler used, manufacturing process and adjustment of composition. The clinker ash comprises the gravel content, sand and silty contents with different proportions by weight. Fig. 2 displays the maximum and minimum void ratios of the six types of clinker ash. The standard test method suitable for gravel was employed to determine the maximum
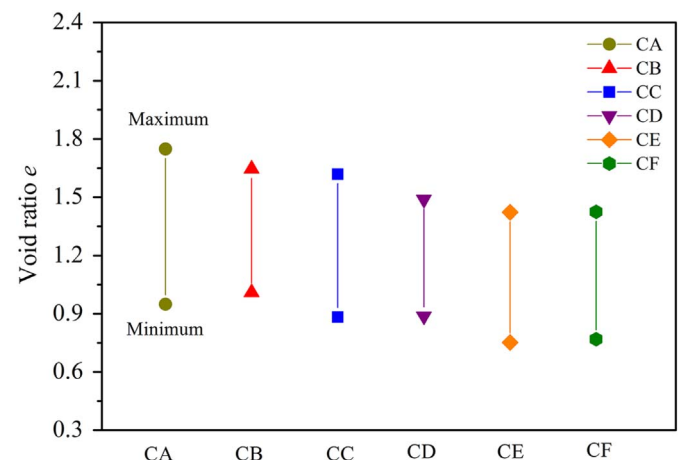
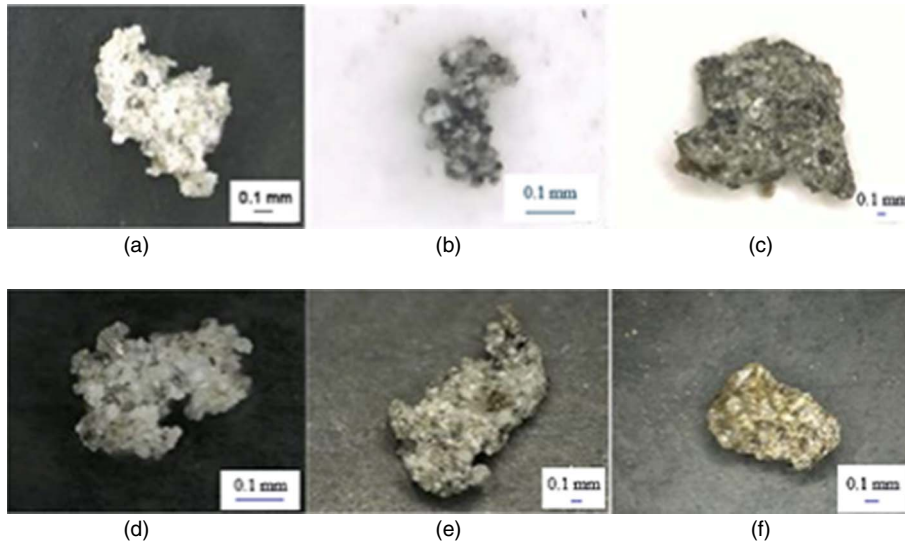Fig. 2. The maximum and minimum void ratios of different types of clinker ash.

Fig. 3. Representative clinker ash grains under electron scanning microscope.

and minimum void ratios because that grains with diameter above 2.0 mm were contained in samples (JIS A 1224, 2009). Clinker ash also has a larger maximum void ratio e_{max} and minimum void ratio e_{min} in comparison with natural sands. This is attributed to the larger void space between grains with complex and angular shapes.

2.2. Particle properties

Fig. 3 a–f shows the representative microscopic photographs of clinker ash grains. The grains alike natural sand and grains with irregularity are seen. From the pictures, the porous nature of particles can be clearly observed. The grains have many pores and these pores are formed when the clinker ash particles fall from the hot incineration boiler (around 1400 °C) into a water tank below where they rapidly cool and harden. Thus, there are pores connected to the surface as well as within the particle itself. Clinker ash particles have very angular and coarser surfaces due to the particles being crushed in a grinder to a maximum diameter of around 2.0 cm. These particle shape features can be thought to have a great influence on the physical, particle and mechanical properties of clinker ash.

Microscopic observation of particles at a stable place was performed using a 1.92-million-pixel camera at a resolution of $1600 * 1200$. Previous study revealed that that taking 20 particles at random from a

sample and then taking the average of the results were sufficient in representing the shape characteristics of a sample (Yoshimura and Ogawa, 1993). Accordingly, 30 particles from each sample from CA to CF were extracted and their particle shape indexes were decided.

2.2.1. Particle shape

Two indexes including aspect ratio A_r and roundness coefficient R_c are employed to describe the particle shape characteristics of clinker ash (Nakata et al., 2001b). The aspect ratio A_r in Eq. (1) is ruled to be the ratio between the longest and shortest dimensions of a particle.

$$A_r = b/a \tag{1}$$

where b and a represent the length of the longest and shortest dimensions of a grain, respectively. The aspect ratio A_r takes the value of 1 when the particle is perfectly spherical. It increases for grains with complex shapes. The other particle shape index, roundness coefficient R_c, can be calculated by Eq. (2)

$$R_c = L^2/4\pi A \tag{2}$$

where L is the circumference of the particle and A is the cross-sectional area. A roundness coefficient R_c closer to 1 indicates that particle shape is closer to a sphere, with higher values indicating more angularity.

Fig. 4 shows the plot of roundness coefficient R_c against the aspect ratio A_r for clinker ash, granulated coal ash and other natural sands (Yoshimoto et al., 2012). The results for natural sands are distributed
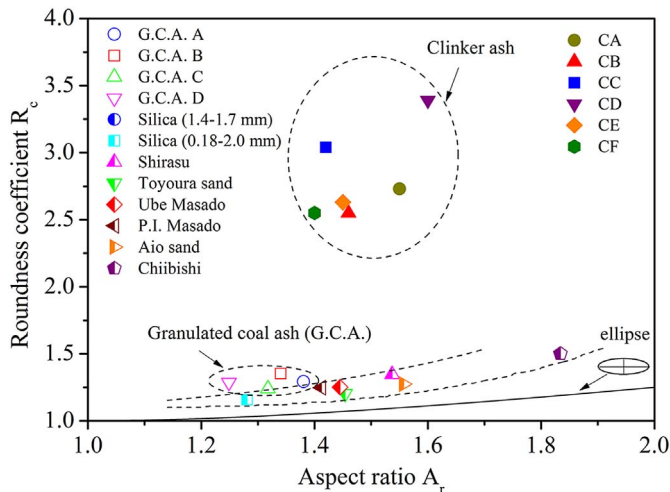

Fig. 4. The roundness coefficient R_c and aspect ratio A_r of clinker ash and other artificial sands and natural sands.
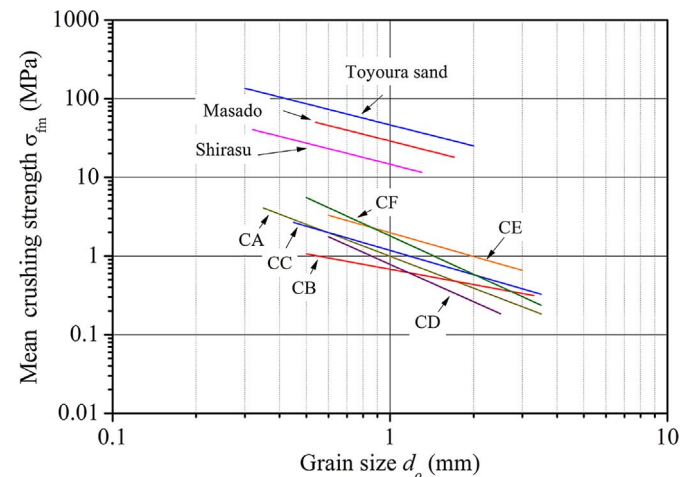

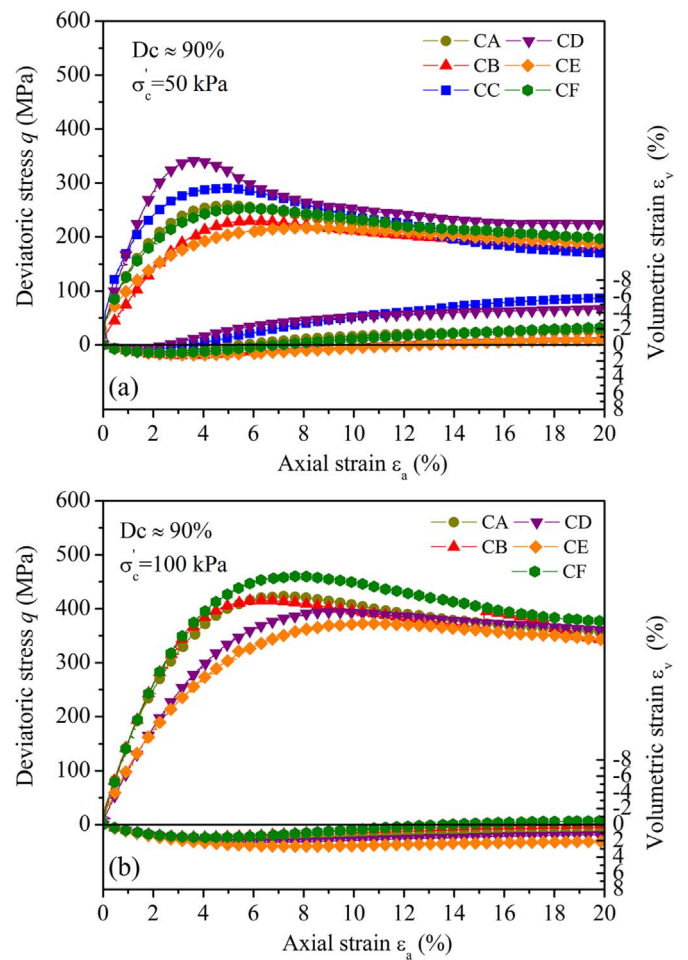**Fig. 5.** The mean crushing strength of clinker ash and other natural sands.

Table 2
The triaxial compression test conditions on clinker ash.

Sample name	σ_c' (kPa)	Target D$_c$ (%)			Sample name	σ_c' (kPa)	Target D$_c$ (%)		
		85	90	100			85	90	100
		Actual D$_c$ (%)					Actual D$_c$ (%)		
CA	50	83.5	88.1	96.9	CD	50	83.6	87.3	
	100		88.0	97.9		100		90.8	100.7
	200	83.4	87.4	99.1		200	85.0		101.4
CB	50	88.1	90.1	103.4	CE	50	84.6	87.7	100.1
	100		92.7	104.2		100	85.0	86.2	102.9
	200	86.0	93.7	104.9		200		90.0	98.0
CC	50	83.8	88.2	96.8	CF	50	85.0	88.9	100.3
	100			98.6		100	85.0	92.0	99.3
	200	83.0		101.0		200	85.0		99.9
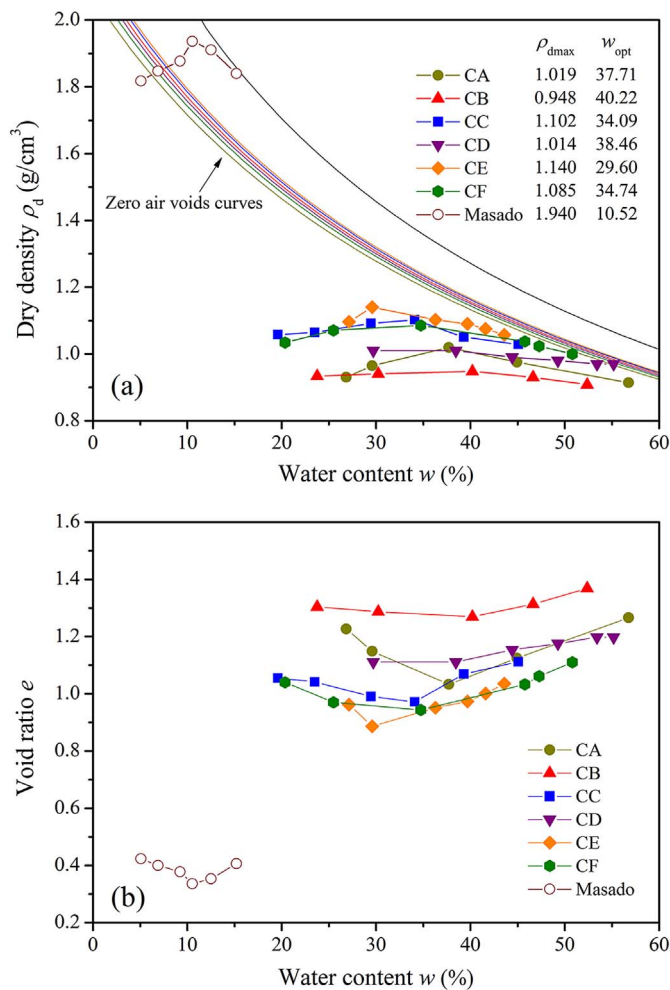
Fig. 6. Variations in the dry density and void ratio of different types of clinker ash with water content (a) Compaction curve (b) void ratio-water content curve.

Fig. 7. Stress-strain relationship of clinker ash with varying particle characteristics and degree of compaction of 90% at different effective confining pressures (a) $\sigma_c' = 50$ kPa and (b) $\sigma_c' = 100$ kPa.

within the region between two broken curves. It is distinctively seen that the points representing the results of clinker ash lie above granulated coal ash and other natural sands. Clinker ash displays much higher roundness coefficient R_c between 2.55 and 3.04 due to its complex and angular particle shapes formed in the smash process of harden block by a grinder. The aspect ratio A_r of clinker ash is located within the region for natural sands such as Toyoura sand, decomposed granite "Masado" and volcanic soil "Shirasu". "Masado" is regarded as one kind of crushable soil. In the Chugoku region of Japan, "Masado", which comes from weathered granite-type rocks, has long been used as

a ground material in embankments and backfills (Hyodo et al., 1998; Murata et al., 1988; Toyota et al., 2004; Wu et al., 2016). "Shirasu" is a pyroclastic sand from the primary indurated deposit.

2.2.2. Single particle crushing strength

Due to the particle features of artificial formation for clinker ash, it is important to understand its particle strength characteristic and compare it with natural sands. The single particle crushing tests were performed on different types of clinker ash to measure the single particle strength. The description of testing apparatus had been given in
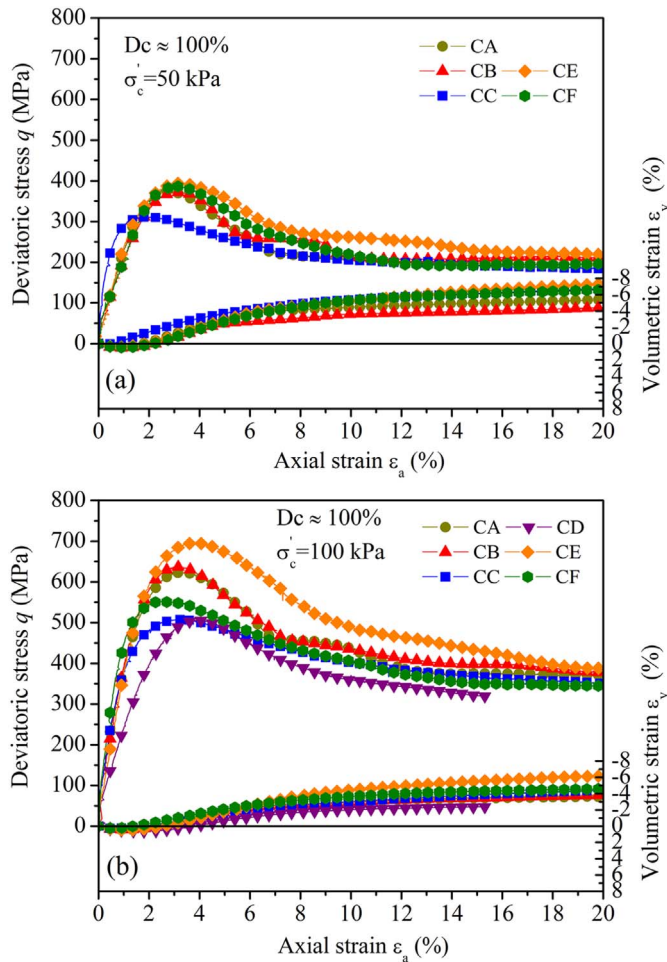
Fig. 8. Stress-strain relationship of clinker ash with varying particle characteristics and degree of compaction of 100% at different effective confining pressures (a) σ_c' = 50 kPa and (b) σ_c' = 100 kPa.

previous study (Nakata et al., 2001a). For each type of clinker ash, 20 particles with different grain diameters were tested. It means that a total number of 60 particles per sample is prepared for testing. A displacement speed of 0.1 mm/min was applied for all the tests.

The crushing strength σ_f is expressed in Eq. (3).

$$\sigma_f = \frac{F_f}{d_0^2} \tag{3}$$

Herein, F_f is the load at failure state and d_0 is the distance between platens in advance of test.

Fig. 5 shows the relationship between the mean crushing stress σ_{fm} and particle size d_0 for clinker ash and other natural sands. The single particle crushing strength takes the average value of the crushing strengths on 20 individual grains. The mean crushing stress for clinker ash is also included in Table 2. For natural sands at the same diameter size, the mean crushing strength decreases in the order of Toyoura sand, decomposed granite "Masado" and volcanic soil "Shirasu". The mean crushing strengths σ_{fm} of natural sands tend to decrease with the increasing particle diameter d_0. The particle with a smaller grain diameter was composed of single mineral and owned a stronger internal structure. It is clearly seen that the mean crushing strengths of clinker ash are lower than natural sands. Test results indicate that clinker ash is a crushable granular material. The grain size dependency of strength for clinker ash is also confirmed and it is in good consistence with previous studies (Nakata et al., 2001a). The slope of the regression line representing the deceasing tendency of mean crushing strength with the rise in diameter size is slightly steeper for clinker ash. It is attributed to

the random distribution of void space in grains and grain structure heterogeneity. In addition, mean crushing stress for each type of clinker ash is also listed in Table 1.

2.3. Compaction properties

The standard proctor compaction tests were carried out in accordance with the specification in (JIS A 1210, 2015). Fig. 6a and b shows the dry density ρ_d and void ratio e plotted against the water content for clinker ash and decomposed granite "Masado". The corresponding maximum dry densities ρ_{dmax} and the optimum water contents ω_{opt} are also presented. The compaction curves of clinker ash exhibit a gentle peak value with the rise in water content and are quite different from the curve of "Masado" with a sharp peak value. The results imply that the dry density ρ_d of clinker ash is less affected by the water content. The difficulty for rearrangement of clinker ash grains with complex and angular shapes is believed to be the primary reason. Accordingly, no special regulation of water content for clinker ash during compaction is required. The zero-air-voids lines for each clinker ash are also depicted.

In addition, dry density ρ_d of clinker ash varying from 0.97 to 1.16 g/cm^3 is much lower than that of "Masado". The implication is that clinker ash is a light-weight material. The optimum water content of clinker ash is between 36% to 48% which is larger than that of "Masao". The possible reason leading to such result is that the water is retained in the air void within grains.

The relative density D_r and degree of compaction D_c are two common indexes to describe the deposition state of geo-materials. The degree of compaction D_c is selected as the indicator to quantify the state of clinker ash in this study due to the following reasons. For crushable soil in dense state, the computed relative density D_r sometimes is over 100% and that contracts its definition. The physical parameters for calculation of relative density D_r are generally determined in dry condition and these parameters are susceptible to the variation in water content. Additionally, the degree of compaction D_c facilitates the density state control for clinker ash as embankment fill material in construction field.

3. Testing preparation

Due to the complex grain surface and existence of pores trapped in grains, it is quite difficult to completely saturate the clinker ash specimens. To ensure the sample was as close to a saturated condition as possible, it was first placed in de-aired water in a vacuum chamber for 2–3 days to remove as much air as possible. The specimen was filtered by water and the back pressure was applied for a whole day to reduce the remained air within specimen in advance of the isotropic consolidation and shearing stages. For each sample, the B-value was checked in advance of shearing and a value larger than 0.95 was obtained. The water pluviation method was employed for clinker ash specimens with the desired degrees of compaction D_c of around 85% and 90%. The target degree of compaction D_c was achieved by tapping the mold using a hammer. It was proved to be problematic for specimens with degrees of compaction D_c = 95% or higher. That was because higher degrees of compaction led to tearing of membrane induced by the sharp and angular clinker ash particles. Thus, a freezing method was adopted to prepare specimens with higher degrees of compaction over 95%. The specimen was first prepared in a separate mold using a 2.5 kg rammer dropped 24 times for each layer from a height of 30 cm, repeated for a total of five layers to attain above compaction energy as gained from compaction tests.

The specimen was 10 cm in height and 20 cm in diameter. Three target degrees of compaction D_c of 85%, 90% and 100% were prepared for specimens to examine the influence of density on shear behaviour. A low-pressure triaxial compression testing apparatus with confining pressure capacity from 50 kPa to 400 kPa was used to perform the
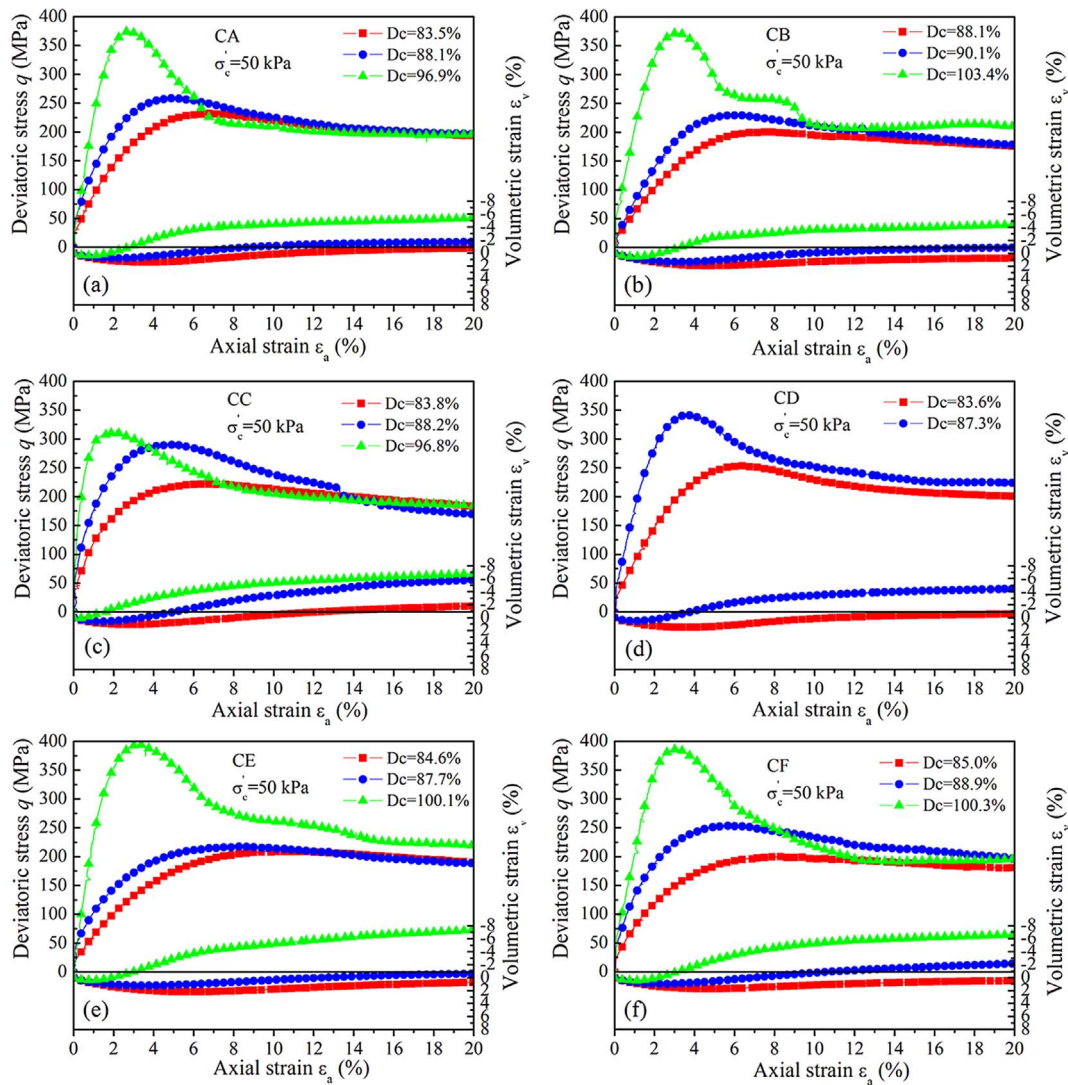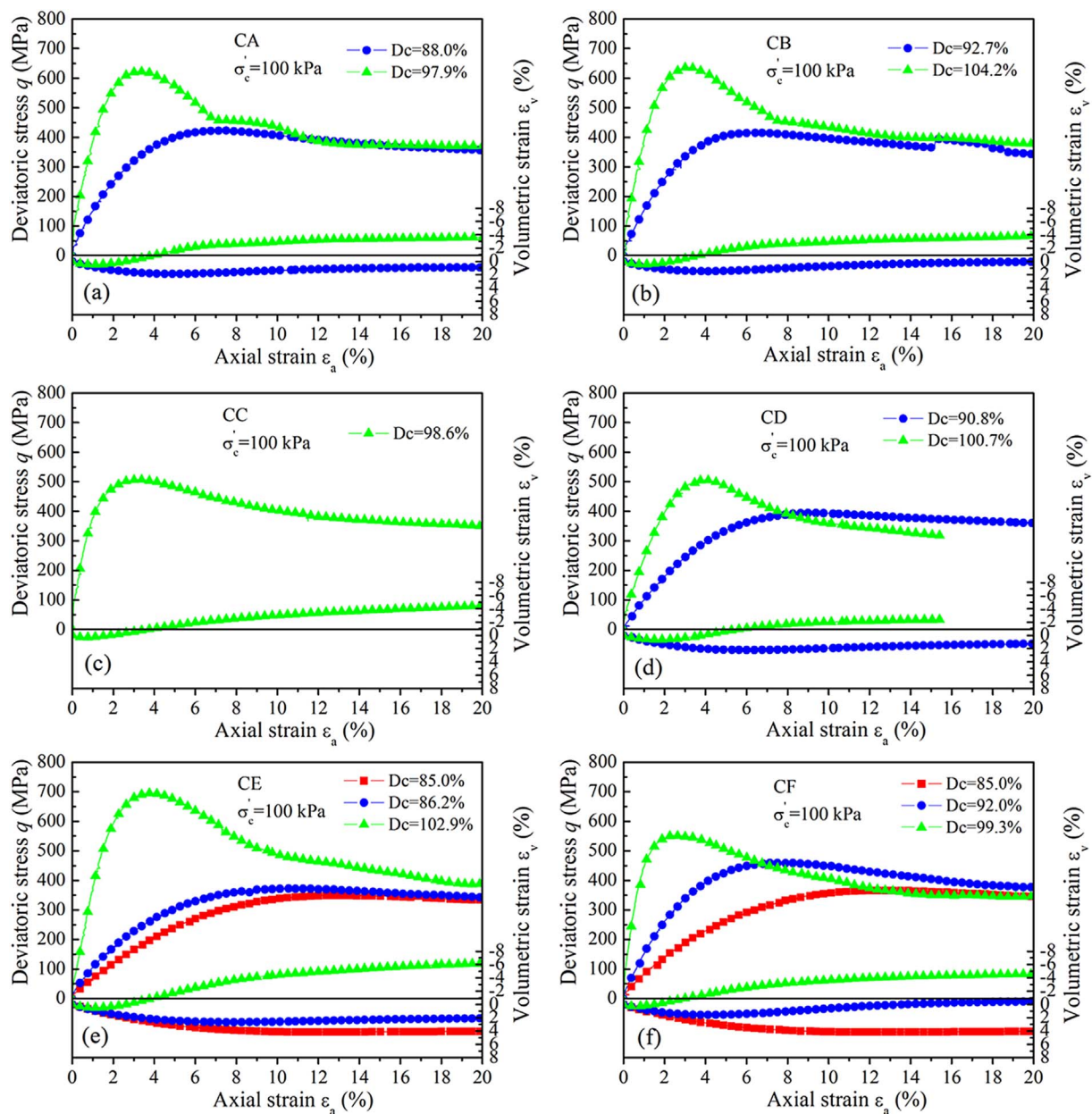
Fig. 10. Influence of degree of compaction Dc on the stress-strain relationship of clinker ash at effective confining pressure of 100 kPa (a) CA (b) CB (c) CC (d) CD (e) CE (f) CF.

stress q, volumetric strain ε_v and axial strain ε_a of drained triaxial tests on all six types of clinker ash with different degrees of compaction D_c at effective confining pressures σ_c' of 50 kPa, 100 kPa and 200 kPa. In each figure, the sub-title a, b, c, d, e and f represent the results of clinker ash CA, CB, CC, CD, CE and CF. It is seen that a rise in degree of compaction D_c significantly increases the initial slope of stress-strain curve and peak shear strength and intensifies the dilation behaviour of clinker ash. The increasing compaction energy also alters the stress-strain curve from strain-hardening or slight postpeak strain-softening behaviour to marked postpeak strain-softening behaviour. Similar results on the influence of degree of compaction on the mechanical behaviour of granular wastes were obtained in past studies (Consoli et al., 2007; Heitor et al., 2016; Kim et al., 2005; Singh and Sharan, 2014). Besides, the increasing degree of compaction D_c decreases the axial strain level at which the peak shear strength occurs. The interlocking mechanism is exerted in dense specimens at an earlier shearing stage. The movement and rearrangement of clinker ash particles at loose state delay the appearance of peak shear strength. Such influences were also reported for

hard-grained and weak-grained sands in previous studies (Lade and Bopp, 2005; Yoshimoto et al., 2016). The deviatoric stresses q of clinker ash converge to a single value as the axial strain progresses at the same effective confining pressure σ_c' regardless of the degree of compaction D_c. The observation of the relatively constant volume state of specimens at larger strains indicates that the critical state (Roscoe et al., 1958) can be reached by clinker ash.

The test results also demonstrate that the increasing effective confining pressure σ_c' at a given degree of compaction D_c enhances the peak shear strength of clinker ash (the range of vertical axis in Figs. 9–11 are different) and leads to a tender strain-softening behaviour. The rise in effective confining pressure σ_c' also alters the deformation behaviour of clinker ash with $D_c \approx 90\%$ from positive dilation to negative dilation due to the occurrence of particle crushing. The great influence of particle crushing on the shear strength and deformation of sands in drained and undrained conditions were examined in past studies (Hyodo et al., 2017, 2002; Shahnazari and Rezvani, 2013; Wu et al., 2013; Yamamuro and Lade, 1996). The shear strength dependence on the confinement
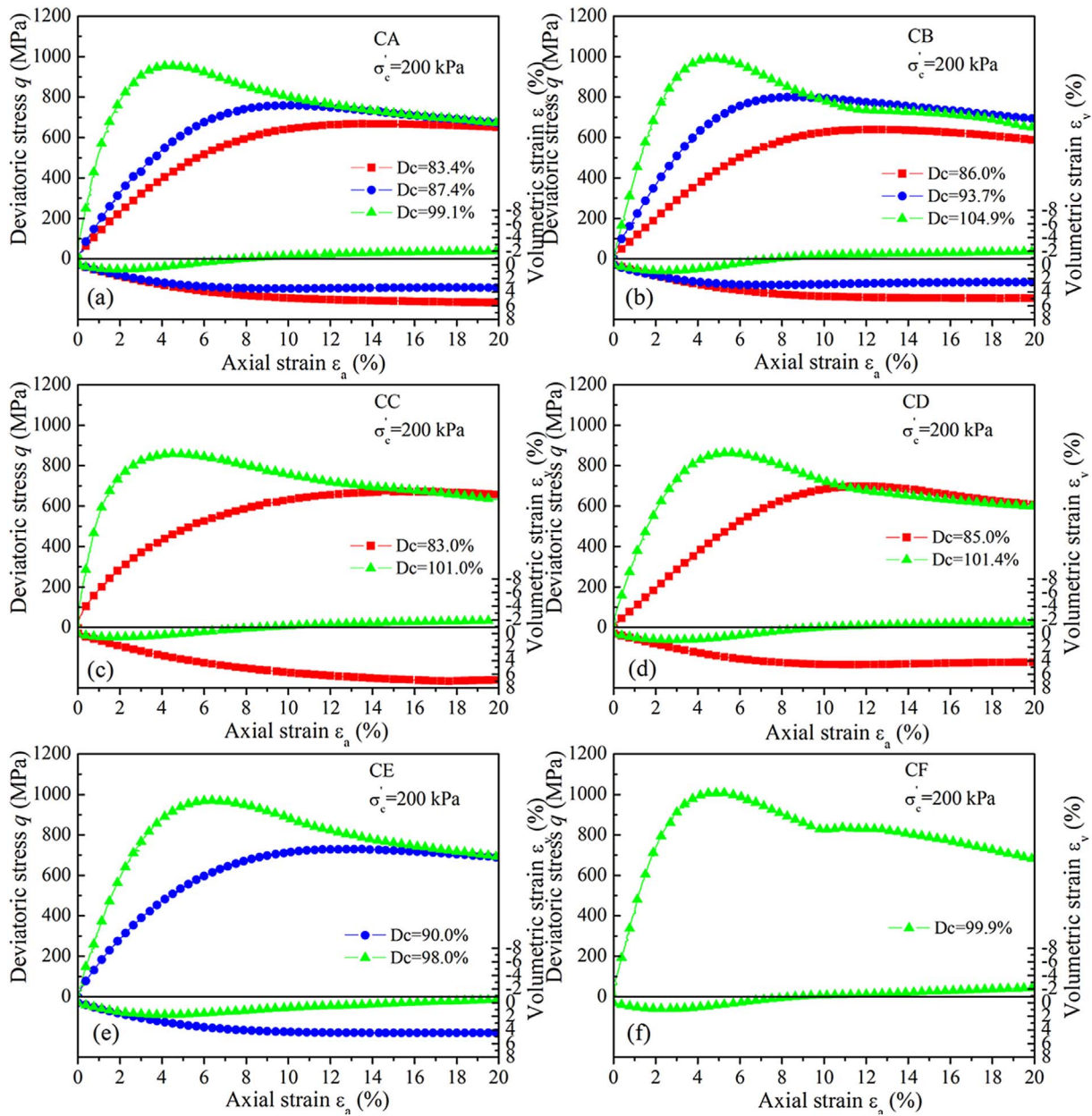
Fig. 11. Influence of degree of compaction Dc on the stress-strain relationship of clinker ash at effective confining pressure of 200 kPa (a) CA (b) CB (c) CC (d) CD (e) CE (f) CF.

stress for clinker ash is confirmed in this experimental investigation.

It is summarized that the shear strength of clinker ash is a complex function of degree of compaction D_c, effective confining pressure σ_c', particle shape parameters and single particle crushing strength σ_f (Winter et al., 2015). From the results presented from Figs. 7–11, the degree of compaction D_c and effective confining pressure σ_c' make a primary contribution to the shear strength for a given type of clinker ash. The particle shape and single particle crushing strength play a secondary role in determining the shear strength. Particle shapes greatly affect the shear strength at relatively lower stresses and the role of single particle crushing strength σ_f in determining the peak shear strength prevails at relatively higher stresses.

Fig. 12 displays the Mohr's circles of representative clinker ash CB and CE with $D_c \approx 100\%$. The secant angle lines of clinker ash at each effective confining pressure σ_c' are drawn. The rise in effective confining pressure σ_c' gradually damages clinker ash grains and ultimately reduces the peak secant angle ϕ_{peak}. Clinker ash approximately loses 7 degree of peak secant angle ϕ_{peak} as the effective confining pressure σ_c'

is raised from 50 kPa to 200 kPa. Besides, one rupture envelope line without passing the origin of the coordinate could be drawn for cohesionless clinker ash at varying effective confining pressures σ_c'. One apparent cohesion value c_d is acquired due to the reduction of peak shear strength originated from particle crushing. The shear strength dependence on the effective confining pressure σ_c' for clinker ash should be fully taken into account in construction field.

Fig. 13 shows the variations in the peak secant angle ϕ_{peak} of all six types of clinker ash with varying levels of effective confining pressure σ_c'. The variations in the peak secant angle ϕ_{peak} with increasing degrees of compaction D_c are displayed in Fig. 14. The test results indicate that the peak secant angles ϕ_{peak} display marked increasing tendency with the decrease in the effective confining pressure σ_c' and rise in degree of compaction D_c. The test results reveal that a peak secant angle ϕ_{peak} over 40° is confirmed for clinker ash with D_c exceeding 90%. A higher peak secant angle over 45° could be acquired for clinker ash with $D_c \approx 100\%$. The higher peak secant angle ϕ_{peak} manifests a higher shear strength. Much higher peak secant angle ϕ_{peak} between 52° and 53° is
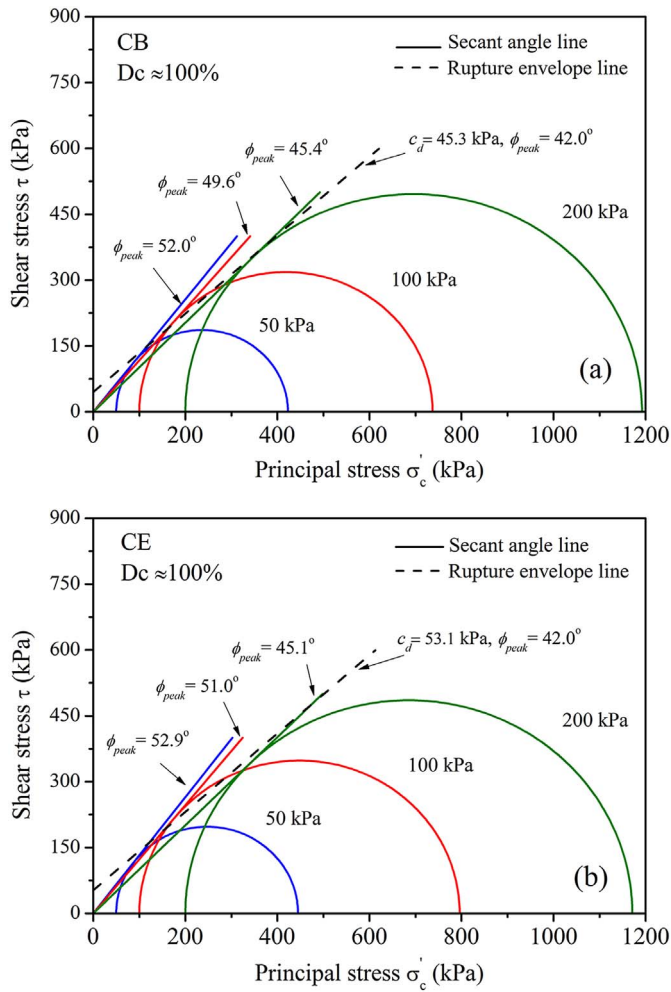
Fig. 12. The Mohr's stress circles of clinker ash CB and CE (a) CB (b) CE.

Fig. 13. The variation in the peak friction angle ϕ_{peak} of clinker ash with varying effective confining pressures (a) Dc ≈ 85% (b) Dc ≈ 90% (c) Dc ≈ 100%.

noticed at a lower effective confining pressure of 50 kPa. The complex and sharp clinker ash grains make a significant contribution to a greater effect of interlocking. The rough surface of clinker ash further increases the inter-particle shear friction and further improves the peak shear resistance.

4.3. A comparison between clinker ash and decomposed granite

To compare the mechanical properties of clinker ash with natural sands, the decomposed granite "Ube Masado" was selected as a reference material. "Masado" is commonly employed as the backfill material for embankment in Japan. Fig. 15 a and b shows the stress-strain relationship of "Ube Masado" and clinker ash CE owing a similar grading curves to "Ube Masado" under the same test conditions. A rise in the degree of compaction D_c significantly enhances the peak shear strength and promotes the dilation behaviour for both of granular materials. Clinker ash CE exhibits a stronger dilation behaviour than "Ube Masado" with the higher degree of compaction D_c at a lower effective confining pressure σ_c'. A marked strain-softening behaviour of clinker ash CE with higher degree of compaction is seen in comparison with "Ube Masado". The shear strengths of clinker ash CE at failure state and the critical state are higher than those of "Ube Masado" in the stresses region tested in this study. Thus, clinker ash has preference to "Masado" as the backfill material due to its higher shear strength. However, the difference in shear strengths between two granular materials decreases with the increasing effective confining pressure σ_c'.
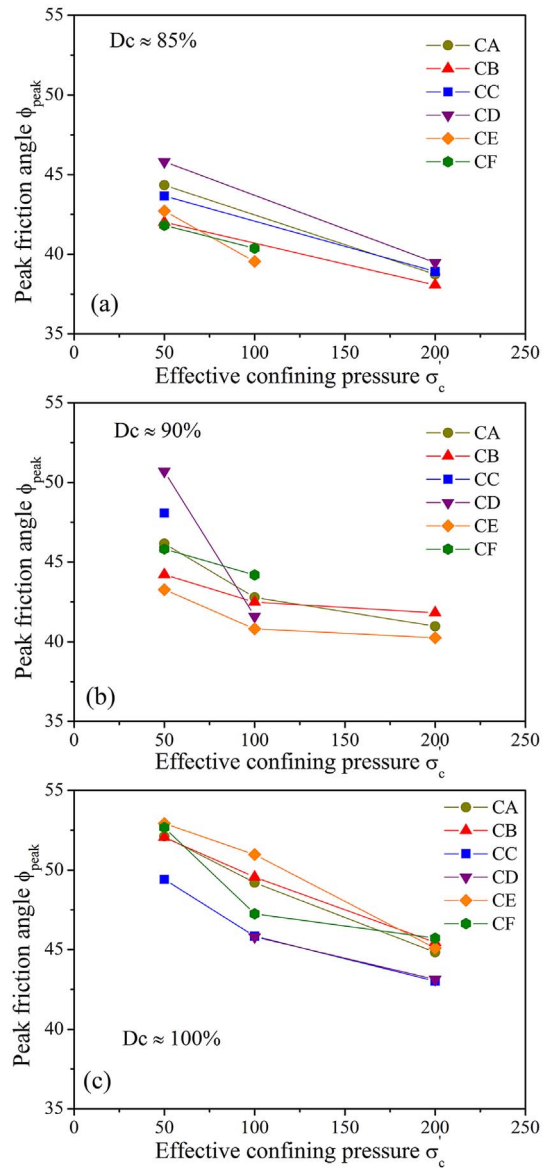
4.4. Stress-dilatancy

Stress-dilatancy relationship describes the evolution of strain rate and stress ratio of soil during shearing. Accurate modeling of the stress-dilatancy relationship is significant to establish the elasto-plastic framework to predict the soil behaviour. Some well-proved expressions were proposed to characterize the stress-dilatancy features of soil in previous examinations (Been and Jefferies, 2004; Guo and Su, 2007; Li and Dafalias, 2000; Nova, 1982; Roscoe et al., 1963; Rowe, 1962; Schofield and Wroth, 1968).

Fig. 16 a and b displays the stress ratio η plotted against the dilation rate D of representative types of clinker ash CA and CF with different degrees of compaction D_c and varying effective confining pressures σ_c'. The stress-dilatancy response at lower stress ratio is not plotted due to some scatter in test data. The dilation rate $D = d\varepsilon_v/d\varepsilon_d$ is employed to examine the stress-dilatancy characteristic of clinker ash. $d\varepsilon_v$ and $d\varepsilon_d$ are the volumetric and deviatoric strain increments, respectively. The results display an initial contraction ($D > 0$) followed by dilation behaviour ($D < 0$). The dilation of clinker ash increases with the rise in degree of compaction D_c. The stress ratio at the peak state η_{peak}
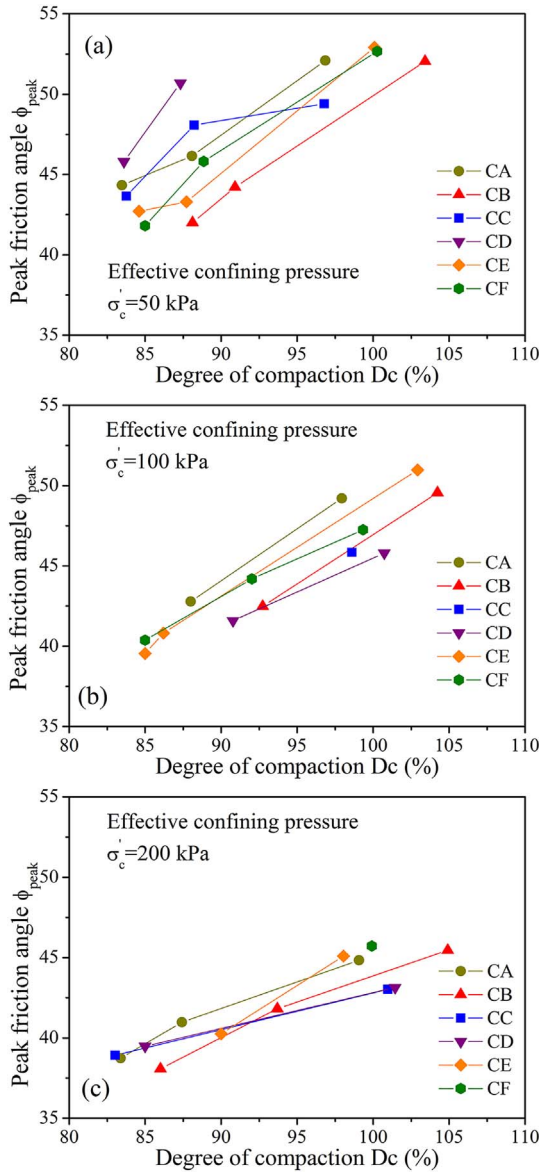
Fig. 14. The variation in the peak friction angle ϕ_{peak} of clinker ash with varying degrees of compaction (a) Dc ≈ 85% (b) Dc ≈ 90% (c) Dc ≈ 100%.

Fig. 15. A comparison on the shear response between clinker ash CE and decomposed granite "Ube Masado" at different effective confining pressures (a) 50 kPa (b) 200 kPa.

corresponds to the minimum result of the dilatancy function D_{min}. The "hook" on the stress-dilatancy curve identified for natural granular materials (Been and Jefferies, 2004) is also observed for clinker ash. The stress-dilatancy behaviour of clinker ash displays the similar pattern and is less dependent on the degree of compaction D_c and level of effective confining pressure σ_c'. A trend line to fit the peak stress ratio η_{peak} and the minimum dilatancy D_{min} on the stress-dilatancy curves using the Nova's rule in Eq. (4) is drawn for clinker ash CA and CF (Nova, 1982).

$$D = (M - \eta)/(1 - N) \qquad (4)$$

where N is a density-independent material property. The Nova rule could be integrated into the Nor-sand model using the void ratio as a model variable (Jefferies, 1993). The Nor-sand model considering the influence of density is in preference to the modified Cam-clay Model (Schofield and Wroth, 1968) in modeling the mechanical response of granular materials. Besides, Nova's stress-dilatancy law examines the trends of peak strength of a larger number of tests rather than the result of a single test. Thus, the flow rule proposed by (Nova, 1982) is employed to assess the dilatancy behaviour of clinker ash in this study. M
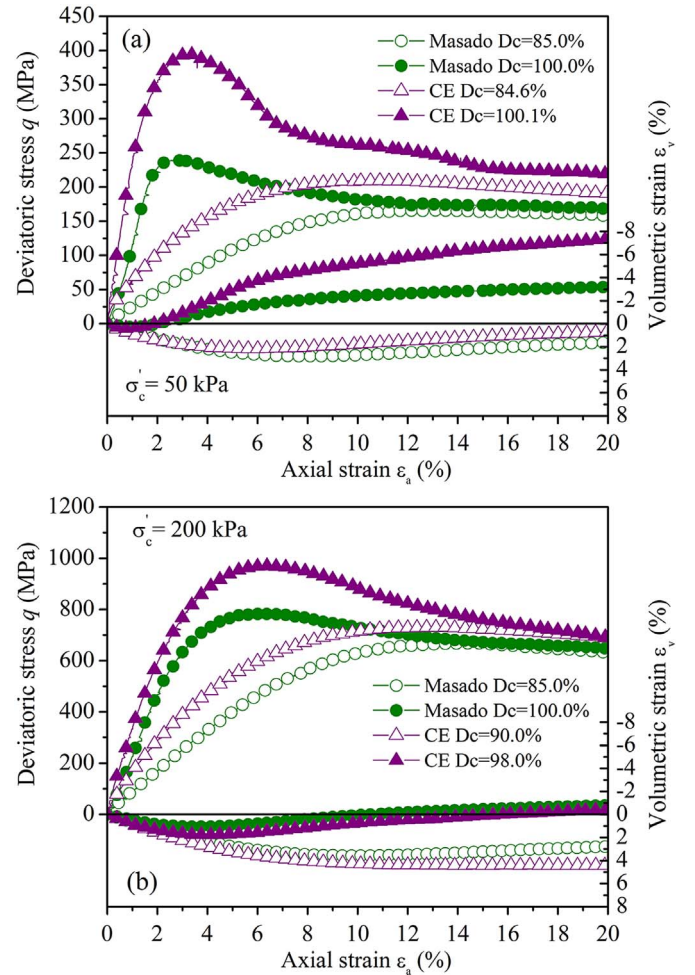
is the stress ratio at the critical state and determined as the intercept in vertical axis of trend line when the dilation rate D is instantaneously zero. There is a strong correlation between critical state stress ratio M and mean crushing stress σ_{fm} for six types of clinker ash in Fig. 17 because these two parameters represent the native features of clinker ash. A larger mean crushing stress produces a larger stress ratio at the critical state.

Fig. 18 presents the $(\eta_{peak} - M)/(1 - N)$ plotted versus D_{min} of all types of clinker ash with different degrees of compaction D_c and the trend lines determined using Nova's rule. N varying from 0.487 to 0.608 for all types of clinker ash is much higher than those of natural sands between 0.2 and 0.3 (Jefferies, 1993). N was also advocated to be an index to assess the crushability of sand and this approach was employed to examine the crushability of similar waste materials, granulated coal ash, in previous studies (Wu et al., 2014; Yoshimoto et al., 2016). A larger N indicates a higher crushability for clinker ash.

4.5. Evolution of critical state line

Fig. 19 a and b shows the stress paths of representative types of clinker ash CA and CF with three degrees of compaction D_c during drained shearing. Multiple critical state lines of clinker ash are identified on the void ratio and logarithm of effective mean stress plane. The critical state line of clinker ash moves downward and towards smaller void ratios with a rise in the degree of compaction D_c. The location of critical state line associated with the compaction energy is in good agreement with the descending of critical state line of compacted coal
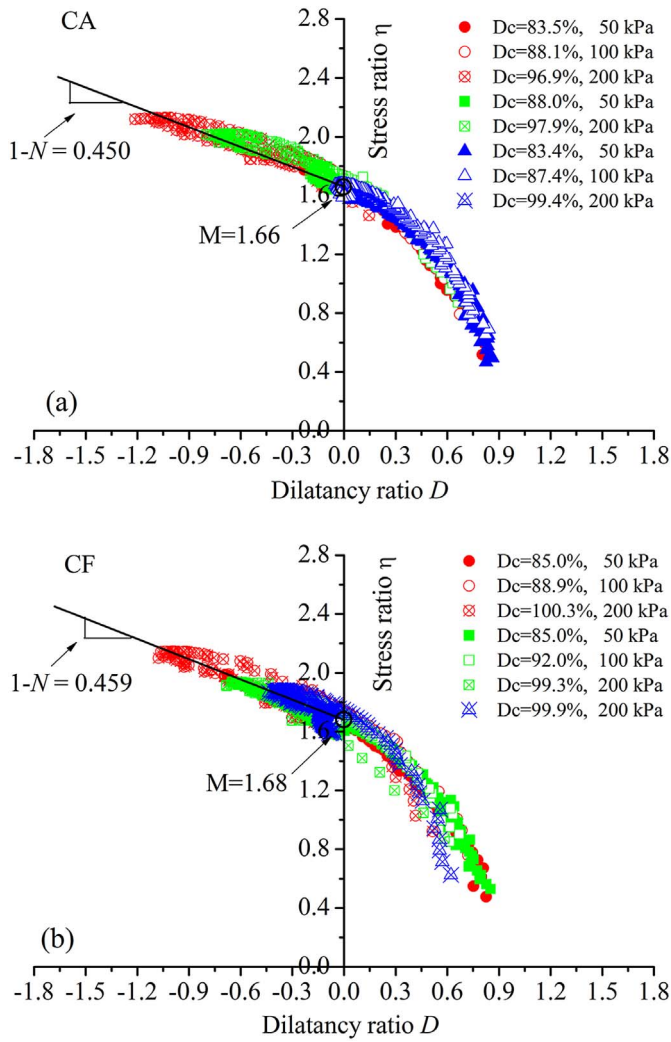
Fig. 16. Stress-dilatancy of clinker ash CA and CF with varying degrees of compaction and at effective confining pressures (a) CA (b) CF.
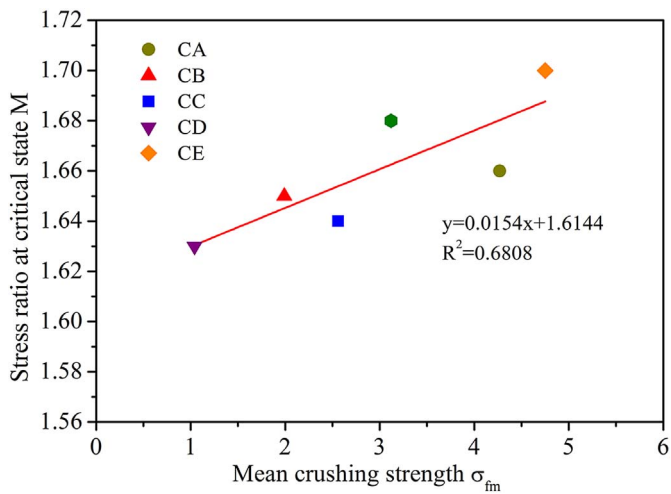

Fig. 17. The relationship between the stress ratio at the critical state *M* and the mean crushing strength for clinker ash.

Fig. 18. The relationship between the stress ratio and dilation rate for clinker ash.
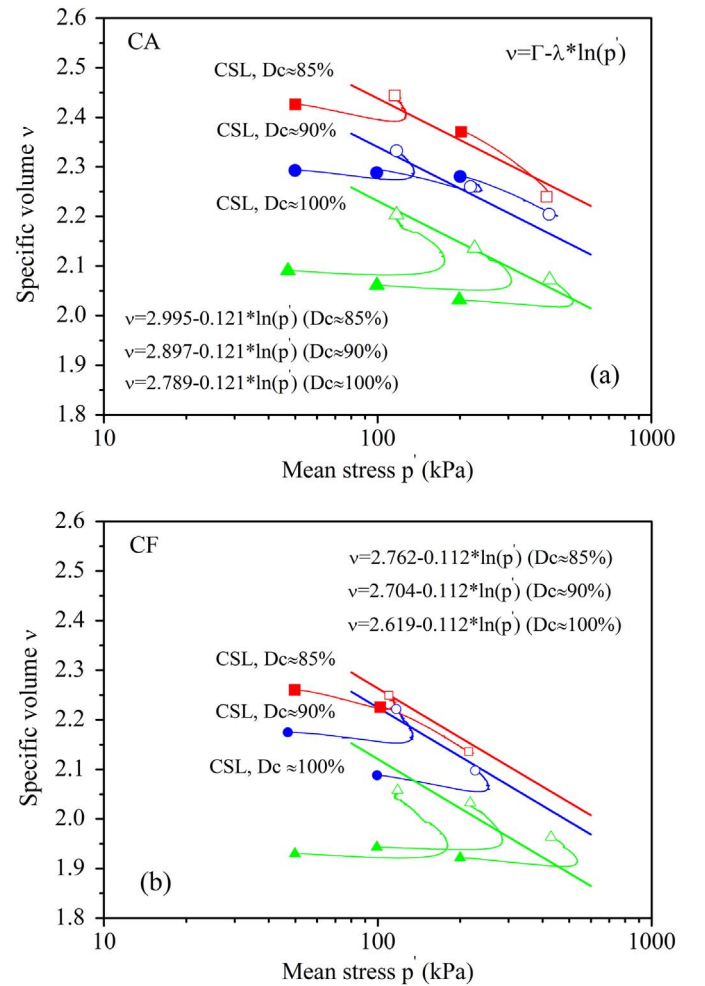
Fig. 19. Identification of the critical state lines of clinker ash with different degrees of compaction (a) CA (b) CF.

wash (Heitor et al., 2016). The amount of particle crushing for clinker ash increases in accompaniment with the increasing degree of compaction. The occurrence of particle crushing produces smaller fines particles and the void spaces are filled. The rise in the amount of

particle crushing during compaction process alters the grain gradation towards to a well-graded distribution in advance of isotropic consolidation and shearing. The movement of critical state lines of granular materials were numerically and experimentally examined in previous studies and the initial gradation of soils was regarded as the governing factor in determining the location of critical state line (Daouadji et al.,

Fig. 20. Identification of the critical state surfaces of clinker ash with different degrees of compaction (a) CA (b) CF.

Fig. 21. Grain size distribution curves of clinker ash CA and CF before and after compaction, shearing testing at different effective confining pressures (Dc ≈ 100%) (a) CA (b) CF.
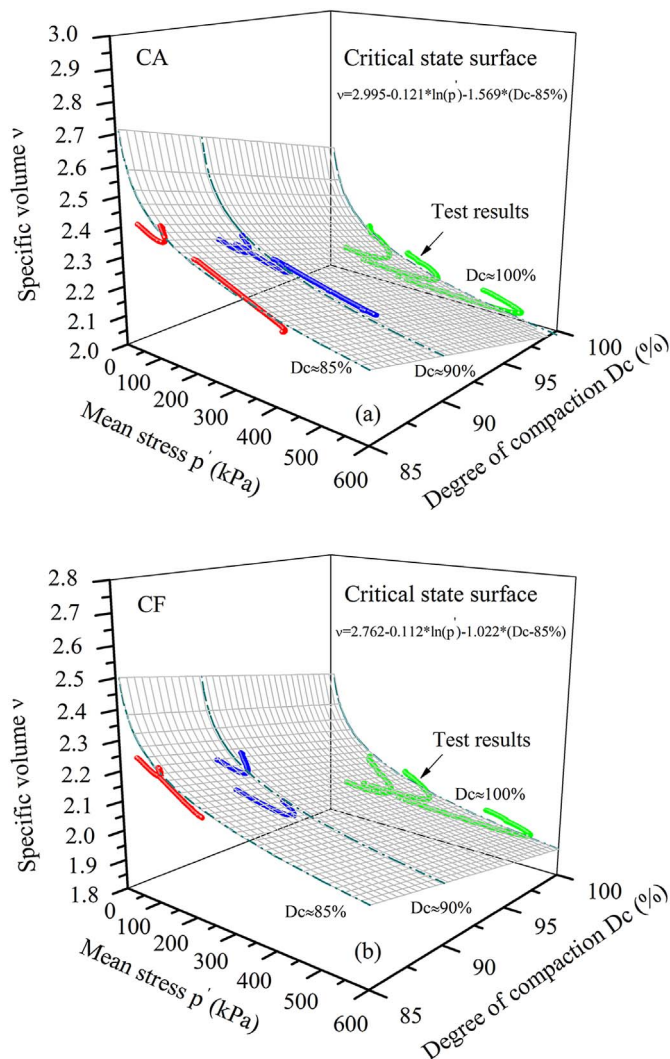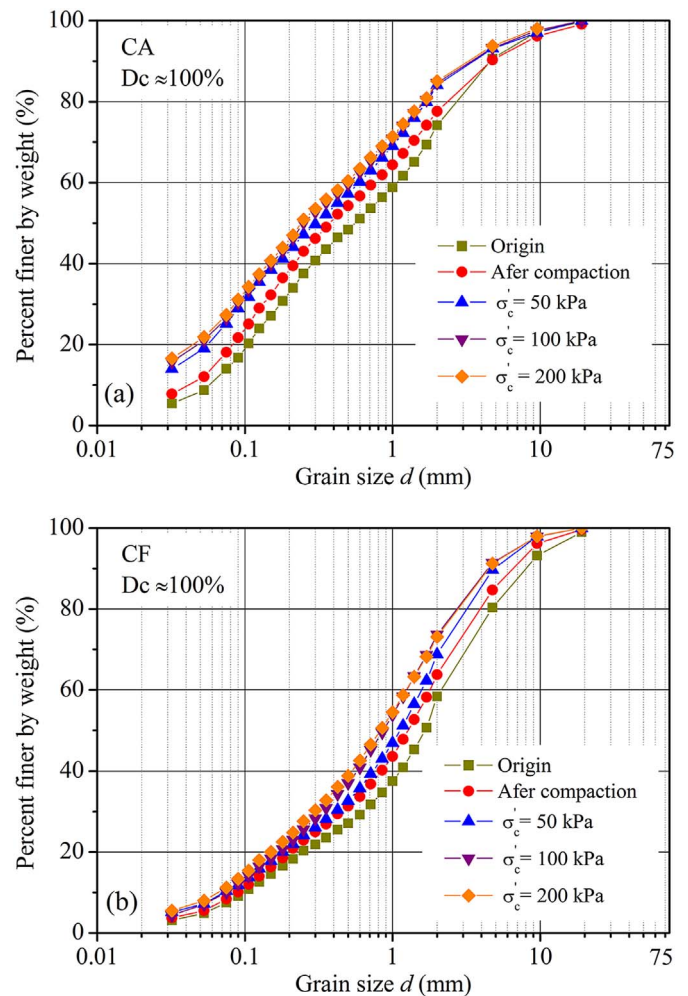
2001; Ghafghazi et al., 2014; Kikumoto et al., 2010; Wood and Maeda, 2008). It was noted that a family of critical state lines of sands existed due to particle crushing and they paralleled to each other. The slope of critical state line of clinker ash is assumed to be independent on the degree of compaction and drawn in accordance with the test results in this examination. Bandini and Coop (2011) and Xiao et al. (2016) also noticed that the shift of critical state line was the result of a combination of vertical movement and rotation. The divergence is probably induced by the different mineralogy composition of the sands tested.

The critical state line is generally expressed in Eq. (5).

$$\upsilon = \Gamma - \lambda \ln p' \qquad (5)$$

where $\upsilon = 1 + e$ is the specific volume, λ is the slope of critical state line and Γ is the intercept of the critical state line when the effective mean stress $p' = 1$ kPa. Fig. 20 a and b displays the critical state surfaces of clinker ash CA and CE in the p-q-υ space (Chiaro et al., 2014).

4.6. Confirmation of particle crushing

To examine the occurrence of particle crushing in the compaction and shearing stages, the grain size distribution curves of one representative type of clinker ash CF before and after the compaction, and after the subsequent shearing at different effective confining pressures were measured. Fig. 21 shows the variation in the grain size

distribution curves of clinker ash. It is seen that an obvious shift of grading curve after the completion of compaction due to the high crushability of clinker ash. The grading curves moves towards to left as the applied effective confining pressure σ_c' is increased from 50 kPa to 200 kPa. It is seen that the marked variation in grain size ranges from 0.3 mm to 2 mm.

A number of particles with grain diameter between 2 mm and 4.75 mm and painted with colors were seeded into the specimens for the triaxial shearing test to investigate how particle crushing occurred. Fig. 22 shows the particles of clinker ash CF under a digital microscope before and after shearing. The painted particles were retrieved for observation again. The specimens containing colored particles were washed in a 0.7 mm sieve and dried in an oven. The color on the grain surface faded after shearing duo to the inter-particle friction. Different crushing patterns described in (Nakata et al., 2001a) are also identified for clinker ash grains. No visible damage for the red grain is watched in Fig. 22a. The splitting of the grain into two sub-grains and much severer damage type characterized by the splitting and the fragments crumbing to power can be seen in Figs. 22b and c.

5. Conclusions

The physical, particle, compaction and mechanical properties of clinker ash were thoroughly studied in this experimental investigation to examine its suitability as a new form of backfill material for retaining wall and embankment. Six representative types of clinker ash with
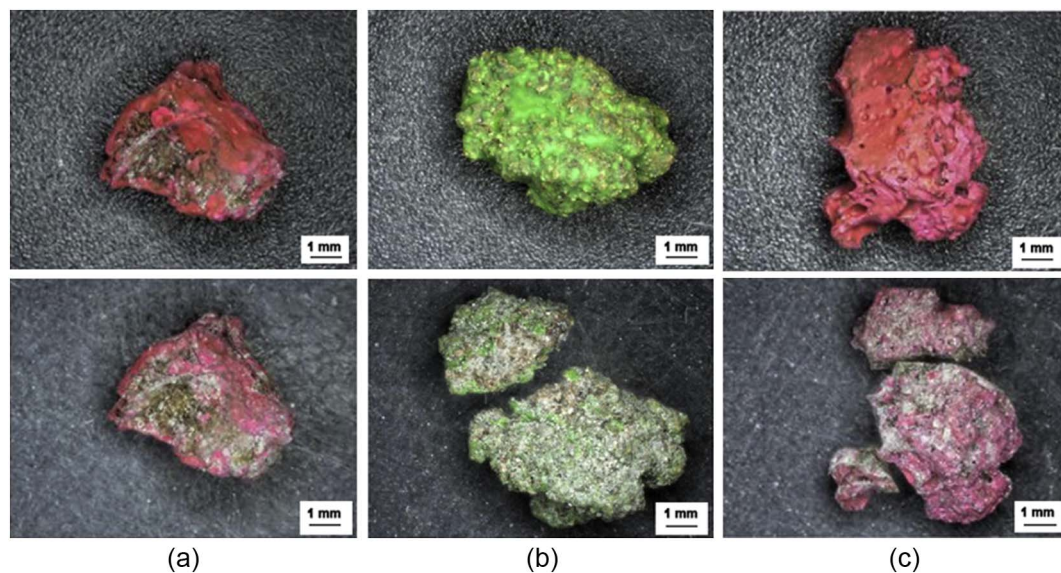
Fig. 22. The appearance of colored particles within the specimen of clinker ash CF before and after shearing (D$_c$ ≈ 90%, σ_c' = 100 kPa).

varying particle characteristics were selected from different thermal power plants located in western Japan. The mean crushing strength of each type of clinker ash with varying grain diameters were measured. The effects of degree of compaction and effective confining pressure on the shear response, stress-dilatancy and critical state characteristics of clinker ash were examined. Clinker ash could be compared favorably with conventional sands in terms of the good solution of disposal problem and cost saving. The main conclusions of this study are drawn below.

1. Clinker ash is one kind of light-weight renewable material and could be cheaply obtained as the by-product from the thermal power plant. The grain size curve of clinker ash is widely distributed and greatly alters with the composition and location site. The compaction curve of clinker ash is gently curved in comparison with other natural sands. Its dry density ρ_d is less susceptible to the variation in water content and this characteristic is advantage for field construction.

2. The mean single particle crushing strength of clinker ash is lower than natural sands and this demonstrates its high crushability in nature. The complex and sharp shapes of clinker ash give rise to larger roundness coefficients and larger differences between the maximum void ratio and minimum void ratio of clinker ash in comparison with natural sands.

3. A peak secant angle over 40° could be obtained when the degree of compaction is 90% or larger and the effective confining pressure is higher than 50 kPa. Clinker ash has a higher peak secant angle even with a lower degree of compaction duo to its sharp and angular shapes. The structure of clinker ash with many angular increases the interlocking effect and further provides a higher shear resistance. The increasing effective confining pressure reduces the peak secant angle caused by the fragment of particles.

4. The rise in the degree of compaction D_c greatly enhances the initial stiffness and peak shear strength and intensifies the dilation behaviour and such tendency is more prominent at a lower effective confining pressure.

5. The degree of compaction and effective confining pressure make a primary contribution to the shear strength of clinker ash. The clinker ash with a larger roundness coefficient such as CD and CC own a larger shear strength at an effective confining pressure of 50 kPa. It indicates that the particle shape plays an influential role in determining the shear strength of clinker ash at lower effective confining pressures. The influence of particle shape on the shear strength is gradually removed as the stress level is increased and the shear strength of clinker ash is more dependent on the single particle strength.

6. The stress-dilatancy curves of clinker ash are less dependent on the degree of compaction and level of effective confining pressure. The stress-dilatancy relationship is also evaluated by the Nova rule. A larger N is obtained and it indicates a higher crushability for clinker ash. A unique stress ratio at the critical state could be determined for a given type of clinker ash and it is closely correlated with its mean crushing strength.

7. The downward movement of the critical state line for clinker ash with the rise in the degree of compaction is identified and this varying tendency is induced by the occurrence of particle breakage. The remarkable particle crushing is evidenced by the variation of grain size distribution curves and the observation of the colored particles before and after shearing.

8. Clinker ash displays similar shear response with that of decomposed granite "Ube Masado" under the similar test conditions and possesses a higher shear strength at the effective confining pressures varying from 50 kPa to 200 kPa applied in this study.

Acknowledgements

References

Arakawa, T., Narita, K., Otaka, M., 2004. Application of clinker ash for soil improvement. Electr. Power Civil Eng. 44–47 (in Japanese).

Bandini, V., Coop, M.R., 2011. The influence of particle breakage on the location of the critical state line of sands. Soils Found. 51, 591–600. http://dx.doi.org/10.3208/sandf.51.591.

Been, K., Jefferies, M., 2004. Stress-dilatancy in very loose sand. Can. Geotech. J. 41, 972–989. http://dx.doi.org/10.1139/t04-038.

Bolton, M.D., 1986. The strength and dilatancy of sands. Géotechnique 36, 65–78. http://dx.doi.org/10.1680/geot.1986.36.1.65.

Chang, A.C., Lund, L.J., Page, A.L., Warneke, J.E., 1977. Physical properties of fly ash-amended soils. J. Environ. Qual. 6, 267–270. http://dx.doi.org/10.2134/jeq1977.00472425000600030007x.

Chiaro, G., Indraratna, B., Tasalloti, S.M.A., 2014. Predicting the behaviour of coal wash and steel slag mixtures under triaxial conditions. Can. Geotech. J. 52, 367–373. http://dx.doi.org/10.1139/cgj-2013-0476.

Chiaro, G., Tasalloti, S.M.A., Indraratna, B., Rujikiatkamjorn, C., 2015. Optimisation of coal wash – slag blend as a structural fill. Proc. Inst. Civ. Eng. 168, 33–44. http://dx.doi.org/10.1680/grim.13.00050.

Consoli, N.C., Heineck, K.S., Coop, M.R., Fonseca, A.V. Da, Ferreira, C., 2007. Coal bottom ash as a geomaterial: influence of particle morphology on the behavior of granular materials. Soils Found. 47, 361–373. http://dx.doi.org/10.3208/sandf.47.361.

Daouadji, A., Hicher, P.Y., Rahma, A., 2001. Elastoplastic model for granular materials taking into account grain breakage. Eur. J. Mech. A Solids 20, 113–137. http://dx.doi.org/10.1016/S0997-7538(00)01130-X.

Ferreira, C., Ribeiro, A., Ottosen, L., 2003. Possible applications for municipal solid waste fly ash. J. Hazard. Mater. 96, 201–216. http://dx.doi.org/10.1016/S0304-3894(02)00201-7.

Ghafghazi, M., Shuttle, D.A., DeJong, J.T., 2014. Particle breakage and the critical state of sand. Soils Found. 54, 451–461. http://dx.doi.org/10.1016/j.sandf.2014.04.016.

Guo, P., Su, X., 2007. Shear strength, interparticle locking, and dilatancy of granular materials. Can. Geotech. J. 44, 579–591. http://dx.doi.org/10.1139/t07-010.

Gutierrez, M.S., 2003. Modeling of the steady state response of granular soils. Soils Found. 43, 93–105. http://dx.doi.org/10.3208/sandf.43.5_93.

Heitor, A., Indraratna, B., Kaliboullah, C.I., Rujikiatkamjorn, C., 2016. Drained and undrained shear behavior of compacted coal wash. J. Geotech. Geoenviron. Eng. 142, 4016006. http://dx.doi.org/10.1061/(ASCE)GT.1943-5606.0001422.

Hyodo, M., Hyde, A.F.L., Aramaki, N., 1998. Liquefaction of crushable soils. Géotechnique 48, 527–543. http://dx.doi.org/10.1680/geot.1998.48.4.527.

Hyodo, M., Hyde, A.F.L., Aramaki, N., Nakata, Y., 2002. Undrained monotonic and cyclic shear behaviour of sand under low and high confining stresses. Soils Found. 42, 63–76. http://dx.doi.org/10.3208/sandf.42.3_63.

Hyodo, M., Wu, Y., Aramaki, N., Nakata, Y., 2017. Undrained monotonic and cyclic shear response and particle crushing of silica sand at low and high pressures. Can. Geotech. J. 54, 207–218. http://dx.doi.org/10.1139/cgj-2016-0212.

Iyer, R.S., Scott, J.A., 2001. Power station fly ash - a review of value-added utilization outside of the construction industry. Resour. Conserv. Recycl. 31, 217–228. http://dx.doi.org/10.1016/S0921-3449(00)00084-7.

Jayaranjan, M.L.D., van Hullebusch, E.D., Annachhatre, A.P., 2014. Reuse options for coal fired power plant bottom ash and fly ash. Rev. Environ. Sci. Biotechnol. 467–486. http://dx.doi.org/10.1007/s11157-014-9336-4.

Jcoal, 2014. National Status Survey on the Coal Ash. Japan Coal Energy Center (in Japanese).

Jefferies, M.G., 1993. Nor-sand: a smile critical state model for sand. Géotechnique 43, 91–103. http://dx.doi.org/10.1680/geot.1993.43.1.91.

JIS A 1204, 2015. Test Method for Particle Size Distribution of Soils. JGS (Japanese Standards Association), Tokyo, Japan, pp. 0131.

JIS A 1210, 2015. Test Method for Soil Compaction Using a Rammer. JGS (Japanese Standards Association), Tokyo, Japan, pp. 0711.

JIS A 1224, 2009. Test Method for Minimum and Maximum Densities of Gravels. JGS (Japanese Standards Association), Tokyo, Japan, pp. 0161.

Kamon, M., Katsumi, T., Sano, Y., 2000. MSW fly ash stabilized with coal ash for geotechnical application. J. Hazard. Mater. 76, 265–283. http://dx.doi.org/10.1016/S0304-3894(00)00203-X.

Kikumoto, M., Wood, D.M., Russell, A., 2010. Particle Crushing and Deformation Behaviour. Soils Found. 50, 547–563. http://dx.doi.org/10.3208/sandf.50.547.

Kim, Y.T., Do, T.H., 2012. Effect of bottom ash particle size on strength development in composite geomaterial. Eng. Geol. 139–140, 85–91. http://dx.doi.org/10.1016/j.enggeo.2012.04.012.

Kim, B., Prezzi, M., Salgado, R., 2005. Geotechnical properties of fly and bottom ash mixtures for use in highway embankments. J. Geotech. Geoenviron. Eng. 131, 914–924. http://dx.doi.org/10.1061/(ASCE)1090-0241(2005)131:7(914).

Lade, P.V., Bopp, P.A., 2005. Relative density effects on drained sand behavior at high pressures. Soils Found. 45, 1–13.

Latifi, N., Marto, A., Rashid, A.S.a., Yii, J.L.J., 2015. Strength and physico-chemical characteristics of fly ash–bottom ash mixture. Arab. J. Sci. Eng. 2447–2455. http://dx.doi.org/10.1007/s13369-015-1647-4.

Lee, C.Y., Lee, H.K., Lee, K.M., 2003. Strength and microstructural characteristics of chemically activated fly ash – cement systems. Strength Microstruct. Charact. Chem. Act. Fly Ash 33, 425–431. http://dx.doi.org/10.1016/S0008-8846(02)00973-0.

Li, X.S., Dafalias, Y.F., 2000. Dilatancy for cohesion less soils. Géotechnique 50, 449–460. http://dx.doi.org/10.1680/geot.2000.50.4.449.

McDowell, G.R., Bolton, M.D., 1998. On the micromechanics of crushable aggregates. Géotechnique 48, 667–679. http://dx.doi.org/10.1680/geot.1998.48.5.667.

METI, 2000. Law for Promotion of Effective Utilization of Resources. Ministry of Economy, Trade and Industry (in Japanese).

Ministry of the Environment, 2000. The Basic Law for Establishing the Recycling-based Society. Ministry of the Environment (in Japanese).

Murata, H., Hyodo, M., Yasufuku, N., 1988. Prediction of stress-strain behaviour of undisturbed "Masado.". Technol. Rep. Yamaguchi Univ. 4, 161–170.

Nakata, Y., Hyodo, M., Hyde, A.F.L., Kato, Y., Murata, H., 2001a. Microscopic particle crushing of sand subjected to high pressure one-dimensional compression. Soils Found. 41, 69–82. http://dx.doi.org/10.1139/cgj-2014-0079.

Nakata, Y., Kato, Y., Hyodo, M., Hyde, A.F.L., Murata, H., 2001b. One-dimensional compression behaviour of uniformly graded sand related to single particle crushing strength. Soils Found. 41, 39–51. http://dx.doi.org/10.3208/sandf.41.2_39.

Nova, R., 1982. A constitutive model for soil under monotonic and cyclic loading. In: Pande, G.N., Zienkiewicz, C. (Eds.), Soils Mechanics-Transient and Cyclic Loading. Chicheste, U.K. pp. 343–373.

Roscoe, K.H., Schofield, A.N., Worth, C.P., 1958. On the yielding of soils. Géotechnique 8, 22–53. http://dx.doi.org/10.1680/geot.1958.8.1.22.

Roscoe, K.H., Schofield, A.N., Thurairajah, A., 1963. Yielding of Clays in States Wetter than Critical. Géotechnique 13, 211–240. http://dx.doi.org/10.1680/geot.1963.13.3.211.

Rowe, P.W., 1962. The stress-dilatancy relation for static equilibrium of an assembly of particles in contact. Proc. R. Soc. Lond. A. Math. Phys. Sci. 269, 500–527.

Schofield, A.N., Wroth, C.P., 1968. Critical State Soil Mechanics. McGraw-Hill.

Shahnazari, H., Rezvani, R., 2013. Effective parameters for the particle breakage of calcareous sands: An experimental study. Eng. Geol. 159, 98–105. http://dx.doi.org/10.1016/j.enggeo.2013.03.005.

Singh, S.P., Sharan, A., 2014. Strength characteristics of compacted pond ash. Geomech. Geoengin. 9, 9–17. http://dx.doi.org/10.1080/17486025.2013.772661.

Toyota, H., Nakamura, K., Kazama, M., 2004. Shear and liquefaction characteristics of sandy soils in triaxial tests. Soils Found. 44, 117–126. http://dx.doi.org/10.3208/sandf.44.2_117.

Trivedi, A., Sud, V.K., 2002. Grain characteristics and engineering properties of coal ash. Granul. Matter 4, 93–101. http://dx.doi.org/10.1007/s10035-002-0114-6.

Wakatsuki, Y., Hyodo, M., Yoshimoto, N., Anai, R., Yoshinaga, Y., Yoshioka, I., Nakashita, A., 2009. Particle characteristics and strength, deformation characteristics of loose clinker ash. Doboku Gakkai Ronbunshuu C 65, 897–914. http://dx.doi.org/10.2208/jscejc.65.897. (In Japanese).

Wang, D., Abriak, N.E., Zentar, R., 2013. Strength and deformation properties of Dunkirk marine sediments solidified with cement, lime and fly ash. Eng. Geol. 166, 90–99. http://dx.doi.org/10.1016/j.enggeo.2013.09.007.

Winter, M.J., Sueshima, T., Yoshimoto, N., Hyodo, M., Nakata, Y., 2015. Effect of particle characteristics on the shear strength of clinker ash. Geotech. Lett. 3, 1099–1104. http://dx.doi.org/10.1680/geolett.13.00027.

Wood, D.M., Maeda, K., 2008. Changing grading of soil: effect on critical states. Acta Geotech. 3, 3–14. http://dx.doi.org/10.1007/s11440-007-0041-0.

Wu, Y., Yamamoto, H., Yao, Y., 2013. Numerical study on bearing behavior of pile considering sand particle crushing. Geomech. Eng. 5, 241–261. http://dx.doi.org/10.12989/gae.2013.5.3.241.

Wu, Y., Yoshimoto, N., Hyodo, M., Nakata, Y., 2014. Evaluation of crushing stress at critical state of granulated coal ash in triaxial test. Geotech. Lett. 4, 337–342. http://dx.doi.org/10.1680/geolett.14.00066.

Wu, Y., Yamamoto, H., Izumi, A., 2016. Experimental investigation on crushing of granular material in one-dimensional test. Period. Polytech. Civ. Eng. 60, 27–36. http://dx.doi.org/10.3311/PPci.8028.

Xiao, Y., Liu, H., Ding, X., Chen, Y., Jiang, J., 2016. Influence of particle breakage on critical state line of rockfill material. Int. J. Geomech. 16, 4015031. http://dx.doi.org/10.1061/(ASCE)GM.1943-5622.0000538.

Yamamuro, J.A., Lade, P.V., 1996. Drained sand behavior in axisymmetric tests at high pressures. J. Geotech. Eng. 122, 109–119. http://dx.doi.org/10.1061/(ASCE)0733-9410(1996)122:2(120).

Yilmaz, Y., 2015. Compaction and strength characteristics of fly ash and fiber amended clayey soil. Eng. Geol. 188, 168–177. http://dx.doi.org/10.1016/j.enggeo.2015.01.018.

Yoon, S., Balunaini, U., Yildirim, I.Z., Prezzi, M., Siddiki, N.Z., 2009. Construction of an embankment with a fly and bottom ash mixture: field performance study. J. Mater. Civ. Eng. 21, 271–278. http://dx.doi.org/10.1061/(ASCE)0899-1561(2009)21:6(271).

Yoshimoto, N., Hyodo, M., Nakata, Y., Orense, R.P., Hongo, T., Ohnaka, A., 2012. Evaluation of shear strength and mechanical properties of granulated coal ash based on single particle strength. Soils Found. 52, 321–334. http://dx.doi.org/10.1016/j.sandf.2012.02.009.

Yoshimoto, N., Wu, Y., Hyodo, M., Nakata, Y., 2016. Effect of relative density on the shear behaviour of granulated coal ash. Geomech. Eng. 10, 207–224. http://dx.doi.org/10.12989/gae.2016.10.2.207.

Yoshimura, Y., Ogawa, S., 1993. A simple quantification method of grain shape of granular materials such as sand. Doboku Gakkai Ronbunshu 436, 95–103. http://dx.doi.org/10.2208/jscej.1993.463_95.